Appl Phys A (2011) 102: 1027–1032
DOI 10.1007/s00339-011-6283-6

Applied Physics A
Materials Science & Processing

Dc current transport behavior in amorphous GeSe films

Doo Seok Jeong · Goon-Ho Park · Hyungkwang Lim · Cheol Seong Hwang · Suyoun Lee · Byung-ki Cheong

Received: 17 October 2010 / Accepted: 22 December 2010 / Published online: 26 January 2011

Abstract The dc electric conduction behavior of amorphous GeSe films sandwiched between the Pt bottom electrode and various counter electrodes (Pt, Cr, and Ti) was examined in a voltage as well as a time domain. The time domain investigation identified time-dependent resistance change and relaxation. The voltage domain analysis revealed that the current transport in these metal-insulator-metal junctions is probably attributed to bulk-limited band-conduction due to delocalized charge carriers.

1 Introduction

Recently, chacogenide materials have attracted great attention as phase-change random access memory (PRAM) devices are regarded to be a strongly promising candidate for the next generation nonvolatile memory [1, 2]. Indeed, PRAM devices based on $Ge_2Sb_2Te_5$ are already partly substituting NAND FLASH memory in the market. Although the very fast technological progress of PRAM devices is already being achieved, the fundamental physics of interesting electrical phenomena in chalcogenides, for instance, current transport in a sub-threshold regime, threshold switching, resistance drift, and ac conductivity behaviors have not been well understood yet.

D.S. Jeong (✉) · G.-H. Park · H. Lim · S. Lee · B.-k. Cheong
Electronic Materials Center, Korea Institute of Science and Technology, 39-1 Hawolgok-dong, Seongbuk-ku, Seoul 136-791, Republic of Korea
e-mail: dsjeong@kist.re.kr

H. Lim · C.S. Hwang
WCU Hybrid Materials Program, Department of Materials Science and Engineering, and Inter-university Semiconductor Research Center, Seoul National University, Seoul 151-744, Republic of Korea

Concerning a mechanism for current transport in chalcogenides, trap-related conduction mechanisms such as the hopping and the Poole–Frenkel mechanisms seem to be frequently employed to account for observed dc conduction. The hopping mechanism describes the hopping of electronic carriers along trap sites so that it deals with localized electrons. In crystalline systems, hopping conduction is supposed to be observed in limited systems such as wide band-gap materials with deep trap levels. However, unlike ordered systems, electron hopping is regarded as a dominant transport mechanism in disordered systems probably due to the large amount of electron trap sites in the systems. As a matter of fact, ac conductivity behavior in disordered systems is estimated to be attributed to hopping charge carriers [3–5]. Indeed, the experimental results of ac conductivity measurements on various amorphous chalcogenides can be well explained by established hopping conduction theories. However, a mechanism for dc conduction in disordered systems seems to be still controversial. Elliot has regarded the dc conduction due to delocalized electrons (band-conduction) as the mechanism [3]. That is, the two distinctive mechanisms for conduction, localized and delocalized electron transports for dc and ac conduction, respectively, contribute to the whole conduction in the systems. In some literature, electron hopping is taken as a mechanism for dc conduction by analogy with ac conduction [4, 6, 7].

The Poole–Frenkel mechanism describes the reduction of electronic trap depth due to the internal electric field, which consequently leads to an increase in the population of "free electrons" in the conduction band [8]. Therefore, the Poole–Frenkel conduction deals with delocalized electrons. When the number of the free electrons released from traps is much higher than that of the intrinsic free electrons, the Poole–Frenkel conduction can be dominant. Otherwise, the transport of the intrinsic free electrons will be only observed.

It is of great importance to understand the current transport behavior in subthreshold regime because this can shed light on some related issues such as threshold switching and subsequent phase-change. Investigating the current transport in a time domain, i.e., transport kinetics, is also important for a better understanding of the transport nature because the information that we can obtain from voltage-domain analysis is limited. In fact, the current transport behavior of amorphous chalcogenides in a time domain needs to be well understood because a resistance drift phenomenon is a critical issue for the long-term stability of PRAM devices.

In this study, we chose amorphous GeSe as chalcogenide materials. GeSe has been found to be a p-type semiconductor [9].

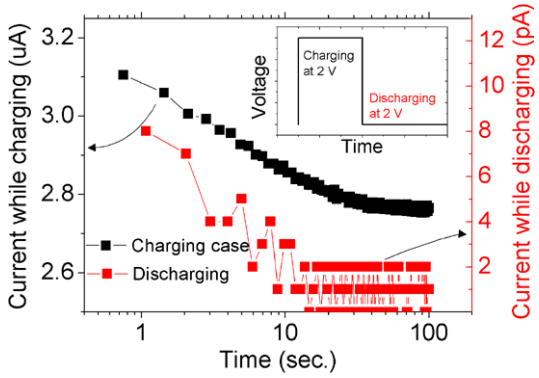

Fig. 1 Current in a time domain for PGP while charging and discharging. The inset depicts the applied voltage profile for the measurement

2 Experiment

Metal-insulator-metal (MIM) junctions including GeSe as an insulator were formed in crossbar structure. Pt bottom electrode was patterned using a lift-off process and deposited using electron-beam evaporation. The thickness of the bottom electrode was 100 nm. An amorphous GeSe film was deposited on the formed bottom electrode in a thermal coevaporator with two separated crucibles for Ge and Se evaporation. The composition of the film was controlled by controlling the flux rate of Ge and Se. The thickness of the GeSe film was 100 nm. The composition of the deposited GeSe film was identified using x-ray fluorescence analysis. The ratio of Ge to Se was found to be approximately unity. Various top electrode materials were subsequently deposited and patterned using the same method as the bottom electrode. Three different junctions, Pt/GeSe/Pt (PGP), Au/Cr/GeSe/Pt (ACGP), and Au/Ti/GeSe/Pt (ATGP) were prepared to identify the effect of electrode materials on the current transport behavior of these junctions. For ATGP and ACGP, Au was deposited on top of Ti and Cr to prevent the oxidation of the oxygen-reactive metals, Ti and Cr, in air. Current-time (I–t) measurement was performed at a fix constant voltage using a Keithley 236 Source Measure Unit, and current-voltage (I–V) behavior at a given delay time was identified with varying sample temperature from 225 to 300 K in a cryostat. The I–V measurement was also done using a Keithley 236 Source Measure Unit.

3 Results and discussion

3.1 Current-time behavior and relaxation

I–t behavior is necessary to be first identified for the correct measurement of I–V behavior. An important parameter of I–V measurement is a delay time of each voltage step in a stair-case voltage sweep. A delay time is set in order to exclude the contribution of displacement current to the measured current. Especially, for high-k materials, the displacement (relaxation) current is quite dispersive in a wide range of a time domain so that one should be careful about setting a proper delay time [10, 11]. Even leakage (dc) current may show dispersive behavior in a time domain, which should be distinguished from displacement current. For instance, dispersive leakage current can be observed in the insulators or semiconductors undergoing the degradation of their resistance under the applied voltage stress.

If a transient current was obsevered at a constant voltage, the origin of the transient current, whether it is displacement or dc current, can be probably judged by some aspects of the current dispersion; the symmetry of charging and discharging currents [12] and the appearance of leakage current when charging current declines below the leakage current [11]. Charging current is supposed to be identical to discharging current so that when one subtracts discharging current from measured overall current, which is the summation of charging and leakage currents, the leakage current can be correctly evaluated; or when the displacement current that decays with time at a given voltage sufficiently below leakage current level, one may observe the true leakage current after all. By these methods, the dc leakage current can be properly extracted from the measured I–t behavior.

Figure 1 shows the I–t behavior of PGP under the applied step-function-like voltage in a time domain ($0 < t < 100$ sec). It can be noticed the difference in I–t behaviors between while charging and discharging so that the current under the voltage is hardly attributed to displacement (relaxation) current. The decrease in the current under the voltage most probably implies an increase in the junction's dc resistance. As a matter of fact, similar observations in amorphous chalcogenides have been frequently reported, which is the so-called resistance drift [13, 14].

The applied constant voltage for the I–t measurement appears to act as voltage stress. And the stress imposed on

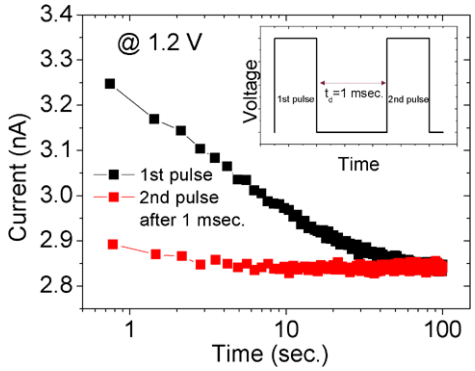

Fig. 2 Transient current of PGP at a voltage of 1.2 V. The lower I–t curve was obtained by applying a second pulse following the first pulse. The time interval between the two pulses was 1 msec. The height of the second pulse was the same as the first one

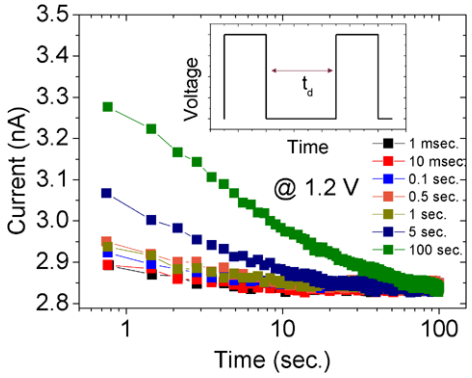

Fig. 3 Transient current of PGP which responded to the second pulse that followed the first pulse after different delay times. The height of the applied voltage pulse was 1.2 V. (1 msec, 10 msec, 0.1, 0.5, 1, 5, 100 sec)

the junction is relaxed as soon as the applied voltage is removed. After a certain time, the junction's resistance recovers its original resistance, meaning stress relaxation. The time constant for the stress relaxation may be quite long. We performed I–t measurement on a pristine junction by applying a step-function-like voltage and subsequent I–t measurement on the stressed junction by applying the same voltage. Figure 2 shows I–t behavior under two voltage pulses of the same pulse height with a time interval (delay time) between them of 1 msec. One can find that a delay time of 1 msec is not enough for the junction to recover the pristine resistance.

Resistance recovery was identified by measuring I–t behavior with various delay times for a subsequent voltage pulse as shown in Fig. 3. From this measurement, it turned out that the recovery time is approximately 100 sec. This implies that the relaxation of the stress imposed by the applied voltage is a phenomenon with a long time constant. At this moment, an exact role of voltage pulses as the source of the stress is hardly understood so that we use the somewhat abstract term "stress." Nevertheless, with the long time constant of the stress relaxation, we can rule out a purely electronic effect as a mechanism for the stress and its relaxation. Indeed, the relaxation time of electrons in semiconductors is much shorter than the observed relaxation time [15]. Especially, for disordered systems containing a large number of traps a relaxation time of approximately 100 sec cannot be explained by means of electronic relaxation.

The time-dependent change in the resistance makes I–V measurement rather complicated. A staircase voltage sweep that is applied for usual I–V measurement will lead to the superposition of the stress induced by various voltages. A delay time in a stair-case voltage sweep is therefore likely to be an important input parameter as will be explained in the next section.

3.2 Current-voltage behavior

Figure 4(a) shows the measured I–V curves for PGP, ACGP, and ATGP samples at two different temperatures (230 and 300 K). As mentioned in the previous section, the delay time is a crucial parameter in I–V measurement. To minimize the voltage stress effect on a junction under test we chose the shortest delay time allowed in our voltage source (1 msec). A double sweep mode was employed to identify the symmetry of the I–V behavior for each junction. In Fig. 4(a), it can be noticed that regardless of the symmetry of the junctions the I–V curves are quite symmetric as can be seen for ATGP and ACGP. In spite of different work functions of Pt, Cr, and Ti [16], the asymmetry of the measured I–V curves is almost negligible. This means that the current transport through each junction barely depends on the band offset at the interface between electrode and GeSe. Furthermore, a current level comparison between each sample as shown in Fig. 4(a) shows a slight difference unlike most of insulating films, whose current transport seriously relies on the Schottky barrier height at the insulator/electrode interface [17, 18]. This aspect is consistent with the symmetry of the I–V behavior in the asymmetric junctions.

In order to understand the current transport mechanism more quantitatively, the current of each junction was measured as a function of temperature under various voltages. Plotting the measured currents against reciprocal temperature on a semilog scale (Arrhenius plot) yields a straight line, implying a single activation energy for the current transport. The activation energy corresponds to energy barrier height for current transport. Since the majority carriers in GeSe are holes, the energy barrier is for holes transport. The Arrhenius plot of measured currents at various voltages for each sample is shown in Figs. 4(b)–(d). Each junction's energy barrier height at different voltages is plotted in Fig. 5(a). As expected, the energy barrier height is found to be independent of the work function of the electrode. Moreover, it

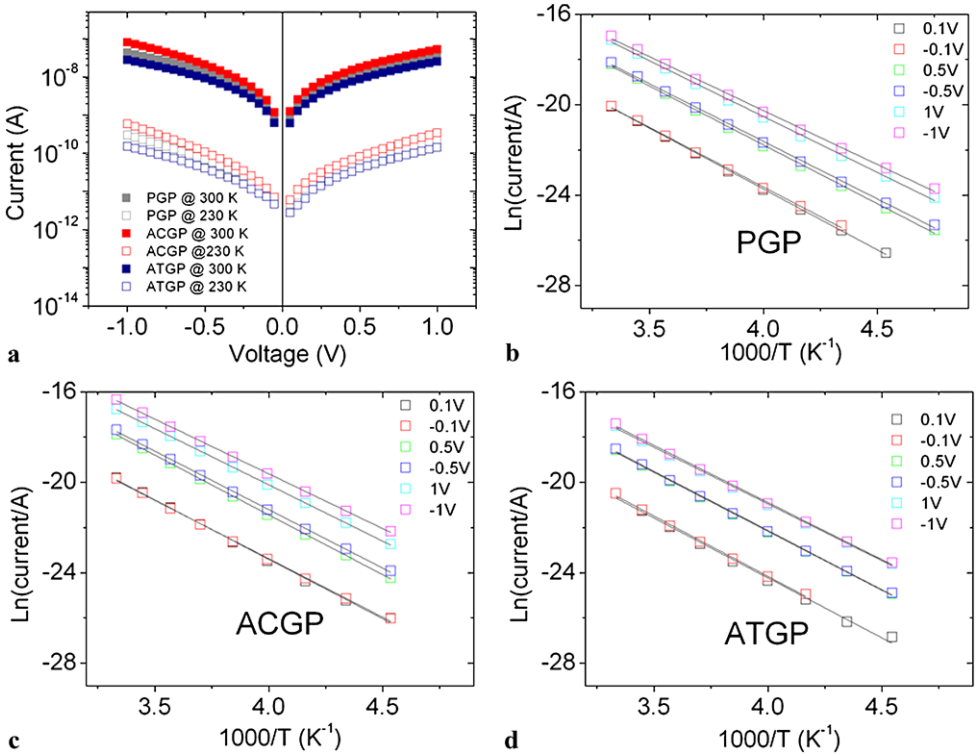

Fig. 4 (**a**) I–V curves of GeSe films sandwiched between various electrodes (Pt, Ti, Cr), which were measured at 230 and 300 K. The Arrhenius plot of currents at various voltages for (**b**) PGP, (**c**) ACGP, and (**d**) ATGP

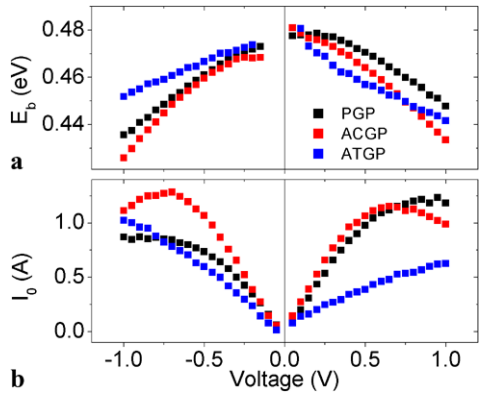

Fig. 5 Evaluated activation energy and pre-exponential factor I_0 for PGP, ACGP, and ATGP by fitting the measured I–V curves using the equation $I = I_0 e^{-E_b(V)/kT}$

can be noticed that the energy barrier height decreases as increasing the applied voltage. The decrease in the energy barrier height implies an increase in the number of the free electrons taking part in current transport.

The I–V curves in Fig. 4(a) can be described as a form of $I = I_0 e^{-E_b(V)/kT}$. I_0, E_b, k, and T are a preexponential factor, energy barrier height, the Boltzmann constant, and lattice temperature, respectively. As discussed earlier, E_b is given by a function of the applied voltage. We extracted E_b and I_0 values at various voltages for PGP, ACGP, and ATGP from I–V curves at various temperatures. The extracted values are plotted in Figs. 5(a) and (b). Figure 5(b) shows an approximately linear I_0–V relationship in a low voltage region for all the junctions. In this voltage region, the nonlinearity of the I–V curves is attributed to the voltage-dependent energy barrier height. However, in a high voltage region, the I_0–V relationship shows a deviation from its linearity in the low voltage region especially for PGP and ACGP. Therefore, in this voltage region, both voltage-dependent barrier height and I_0 are in charge of the nonlinearity.

A general description of particle flux is expressed by $J = cv$, where c and v denote particle concentration and velocity, respectively. For the band-conduction of electronic carriers, v is given by the product of the carrier mobility μ and the electric field E so that $J = c\mu E$. c is thermally activated so that the thermal excitation of current is attributed to c. Concerning the thermally activated c, $c = c_0 e^{-E_b/kT}$, a current conduction equation for band-conduction is expressed as $I = qAc_0\mu E e^{-E_b/kT}$, where q and A are the elementary charge and junction area, respectively. Comparing this equation with the mathematical form used in the analysis on the measured I–V curves, $I = I_0 e^{-E_b(V)/kT}$, gives $I_0 = qAc_0\mu E$. That is, I_0 is proportional to E. If we take an average electric field E_{av} as E in the equation, I_0 is in linear relationship with V, which is indeed what we observed in the low voltage region as discussed in the previous paragraph. This means that the electrons contributing to dc conductivity are accelerated by the applied electric field. However, the mobility of hopping charge carriers is unlikely to be affected by an applied electric field. Although a possible increase in hopping conductivity by an electric

field has been introduced [19], this model cannot account for the observed increase in the mobility by the electric field. A dominant conduction mechanism in the junctions is therefore assumed to be band-conduction (delocalization) rather than electron hopping (localization). E_{av} is not always likely to be identical to E for insulator or semiconductor including a high density of space charges [18]. According to the valence-alternation-pair model [20], in chalcogenides positively- and negatively-charged chalcogens with a three-fold-coordinated C_3^+ and a singly coordinated C_1^-, respectively, serve as space charges. And the concentration of the space charges is of the order of 10^{19} cm^{-3}, for which electric field screening effect on electric field distribution in chalcogenides is not negligible [21]. This may be the reason for the nonlinear I_0–V relationship in the high voltage region in Fig. 5(b).

The measured I–V curves were re-plotted on J/E_{av} versus $E_{av}^{1/2}$ planes for fitting the I–V curves using the Poole–Frenkel conduction mechanism (not shown here). In a certain $E_{av}^{1/2}$ ranges, the curves show linearity, however, the optical dielectric constant that can be extracted from the plot was hardly realistic (>15). The reason why the Poole–Frenkel conduction involves an optical dielectric constant has been explained [22]. In fact, the linearity itself of I–V behavior on the plane for Poole–Frenkel fitting hardly verifies a mechanism for the behavior unless the parameters obtained from the fitting are reasonable. We therefore estimate that the observed I–V behavior does not arise from the Poole–Frenkel conduction.

Current transport through an MIM junction most probably comprises three current terms: injection, bulk, and ejection currents [23]. These three contributions are equivalent to three resistors in a serial connection. Depending on what equivalent resistor among these three terms has the highest resistance, the general conduction equation falls into different conduction mechanism categories. As observed in PGP, ACGP, and ATGP, the energy barrier height for current transport barely depends on electrode materials in spite of their remarkably different work functions. At this moment, a detailed mechanism for the conduction in our junctions is not well understood. Nevertheless, it can be judged that the injection current hardly limits the I–V behavior by our observation that the activation energy for each junction is independent of the Schottky barrier height at the anode/p-type GeSe interface. Therefore, we can assume that the current transport in our junctions is controlled by the bulk of the GeSe films, implying bulk-limited current transport.

The current scaling with the thickness of a GeSe film also demonstrates strong evidence for bulk-limited current transport. For the identification of the current scaling, we prepared MIM junctions with different thicknesses of a GeSe film (60, 80, 100, and 150 nm) and measured their I–V behavior. Figure 6 depicts the measured I–E_{av} curves for

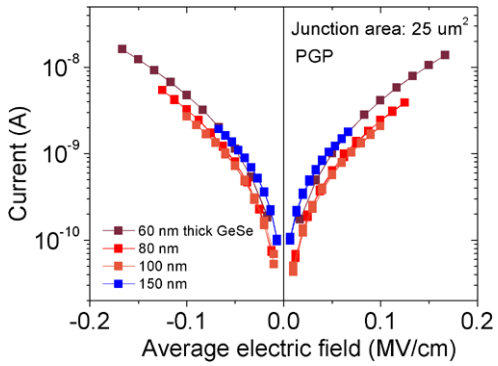

Fig. 6 Current versus average electric field plot for 60, 80, 100, and 150 nm thick GeSe films in PGP samples

the four junctions, where the different I–V behaviors fall into approximately a single I–E_{av} behavior. This implies the current scaling with the thickness. For interface-limited current transport, the current barely scales with the thickness because the Schottky barrier height is given by a function of the electric field at the interface rather than the average electric field [17]. In systems containing a number of space charges, the interfacial electric field should be different from the average electric field as discussed earlier.

These experiments raise the question, "Why is the current through our junctions limited by the bulk?" This question is equivalent to the question, "Why is the injection current high enough not to serve as a bottleneck for the current transport?" To seek the answer to these questions, taking a close look at the anode/GeSe interface using theoretical methods may be necessary. One possible answer to the question is the formation of an Ohmic contact at the interface. However, the evidence identifying an Ohmic contact has not been provided yet. Therefore, the nature of the interface needs to be clarified. Other open questions are about the time-dependent current transport. The understanding of current transport in a time domain should be made prior to that in a voltage domain. Voltage domain analysis on the time-dependent current transport indeed includes time domain analysis on the transport under varied voltages. This means that the voltage domain analysis deals with two variable, time and voltage, which causes further complications.

The effect of voltage stress on the current transport as well as a mechanism for the stress relaxation is barely clarified at the moment. The evaluation of a time-dependent electron band profile in the junctions under the applied voltage would be very helpful for a better understanding of the time-dependent current transport. Since conduction in our junctions seems to be due to band-conduction, internal electric field distribution in the junctions, which is also time-dependent, may be a crucial factor influencing the current conduction. The distribution can be obtained by evaluating the electron band profile.

4 Conclusion

I–t measurement on GeSe junctions shows dispersive current behavior in the time domain, meaning the dc resistance is given by a function of time. We also observed the relaxation of stress imposed on our junctions by the applied voltage. Amorphous GeSe films were assumed to show bulk-limited band-conduction behavior regardless of electrode materials (Here, Pt, Cr, and Ti). From I–V measurement at various temperatures we could obtain voltage-dependent activation energy for the current conduction. Moreover, we found that the preexponential factor of an I–V fitting equation is proportional to the applied voltage in a low voltage region, which may imply the voltage-accelerated velocity of the holes in our junctions. These observations are most likely evidence of band-conduction in our junctions. No dependence of the I–V behavior on electrode materials probably implies bulk-limited conduction. Bulk-limited conduction was double-checked by identifying current scaling with the thickness of a GeSe film.

Acknowledgements This research was supported by a grant from the Fundamental R&D Program for Core Technology of Materials funded by the Ministry of Knowledge Economy, Republic of Korea. We would like to acknowledge a research grant by Korean Ministry of Education, Science, and Technology through an institutional research program of Korea Institute of Science and Technology. CSH acknowledges the support from the World Class University program through the Korea Science and Engineering Foundation funded by the Ministry of Education, Science, and Technology (R31-2008-000-10075-0), Republic of Korea.

References

1. M. Wuttig, N. Yamada, Nat. Mater. **6**, 824 (2007)
2. W.Y. Cho, B. Cho, B. Choi, H. Oh, S. Kang, K. Kim, K. Kim, D. Kim, C. Kwak, H. Byun, Y. Hwang, S. Ahn, G. Jung, H. Jung, K. Kim, IEEE J. Solid-State Circuits **40**, 293 (2005)
3. S.R. Elliott, Adv. Phys. **36**, 135 (1987)
4. M. Mirsaneh, E. Furman, J.V. Ryan, M.T. Lanagan, C.G. Pantano, Appl. Phys. Lett. **96**, 112907 (2010)
5. K. Shimakawa, Philos. Mag. B **46**, 123 (1982)
6. H.S. Metwally, Physica B, Condens. Matter **292**, 213 (2000)
7. H. Sakata, N. Nakao, J. Non-Cryst. Solids **163**, 236 (1993)
8. J. Frenkel, Phys. Rev. **54**, 647 (1938)
9. S. Asanabe, A. Okazaki, J. Phys. Soc. Jpn. **15**, 9 (1960)
10. J.-P. Manceau, S. Bruyere, E. Picollet, M. Minondo, C. Grundrich, D. Cottin, M. Bely, in *IEEE International Conference ICMTS 2006* (2006)
11. E. Bouyssou, P. Leduc, G. Guegan, R. Jerisian, J. Phys. Conf. Ser. **10**, 4 (2005)
12. G.W. Dietz, R. Waser, Integr. Ferroelectr. **9**, 317 (1995)
13. D. Ielmini, A.L. Lacaita, D. Mantegazza, IEEE Trans. Electron Devices **54**, 308 (2007)
14. I.V. Karpov, M. Mitra, D. Kau, G. Spadini, Y. Kryukov, V.G. Karpov, J. Appl. Phys. **102**, 124503 (2007)
15. C.-T. Sah, Proc. IEEE **55**, 654 (1967)
16. V.S. Formenko, *Handbook of Thermionic Properties* (Plenum, New York, 1966)
17. H. Schroeder, S. Schmitz, Appl. Phys. Lett. **83**, 4381 (2003)
18. J.D. Baniecki, R.B. Laibowitz, T.M. Shaw, C. Parks, J. Lian, H. Xu, Q.Y. Ma, J. Appl. Phys. **89**, 2873 (2001)
19. C. Gang, H.D. Koppen, R.W. van der Heijden, A.T.A.M. de Waele, H.M. Gijsman, F.P.B. Tielen, Solid State Commun. **72**, 173 (1989)
20. M. Kastner, D. Adler, H. Fritzsche, Phys. Rev. Lett. **37**, 1504 (1976)
21. R.C. Frye, D. Adler, Phys. Rev. B **24**, 5812 (1981)
22. D.S. Jeong, H.B. Park, C.S. Hwang, Appl. Phys. Lett. **86**, 072903 (2005)
23. J.D. Baniecki, T. Shioga, K. Kurihara, N. Kamehara, J. Appl. Phys. **94**, 6741 (2003)